NTNU – Trondheim
Norwegian University of
Science and Technology

Numerical Investigation of a Post-tensioned Flat Slab with Steel Fibre Reinforcement

Stine Maria F Jensen

Civil and Environmental Engineering
Submission date: December 2013
Supervisor: Jan Arve Øverli, KT

Norwegian University of Science and Technology
Department of Structural Engineering

Department of Structural Engineering
Faculty of Engineering Science and Technology
NTNU- Norwegian University of Science and Technology

ACCESSIBILITY

MASTER THESIS 2013

SUBJECT AREA:	DATE:	NO. OF PAGES:
Concrete Structures	20.12.2013	42

TITLE:

Numerical Investigation of a Post-Tensioned Flat Slab with Steel Fibre Reinforcement

Numerisk undersøkelse av etterspent flatdekke med stålfiberarmering

BY:

Stine Maria Frøiland Jensen

SUMMARY:

This study consists of a numerical investigation of a post-tensioned flat slab without conventional longitudinal reinforcement; only steel fibres were employed to ensure sufficient ductility and shear capacity of the slab. Results were taken from a reported experiment conducted on a full scale steel fibre-reinforced flat slab (0.38 % fibre content) which was tested until failure, undergoing a ductile bending failure at a load of 6.5 kN/m^2. A nonlinear finite element analysis was employed to study the experiment, including the ultimate state. A parametric study was performed using the numerical model to investigate the influence of the tensile behaviour of steel fibre-reinforced concrete (SFRC) the response of the structure. The model proved to be relatively sensitive to changes in the tensile behaviour, but the differences were not prominent until entering the nonlinear area of the load-displacement curve. A constant curve with tensile stress equal to the residual tensile strength of the SFRC provided a robust numerical model and results on the conservative side. Including a peak stress with a multilinear tensile curve provided a less stable analysis but more accurate results. However, the model behaviour was stiffer than the experiment, providing too small deformations at failure. Nevertheless, the numerical model was able to display the ductile bending failure mode and moment redistribution.

RESPONSIBLE TEACHER: Jan Arve Øverli

SUPERVISOR(S): Jan Arve Øverli

CARRIED OUT AT: Department of Structural Engineering

Preface

This Master's thesis was written at the Department of Structural Engineering at the Norwegian University of Science and Technology in Trondheim, during the autumn 2013.

The thesis consists of a numerical investigation of a post-tensioned flat slab with steel fibre reinforcement. The basis for the numerical investigation is a reported experiment conducted on a full scale flat slab that was loaded until failure, and this study constitutes a verification of the experiment.

I chose this assignment because it provided the rare opportunity of performing numerical analyses of an actual full scale experiment, including ultimate limit state. Furthermore, fibre reinforcement is a relatively new and innovative technology, particularly for application in load carrying structures, which makes it an interesting topic.

The thesis is written as a scientific paper. Together with my supervisor, Jan Arve Øverli, it was decided to write a paper to be submitted for the Concrete Innovation Conference 2014 (CIC2014). The length of the paper was limited to 10 pages (in this version the size of the paper is scaled up to fit the B5 format). This report also includes a literature study that covers the background and basic theory of fibre-reinforced concrete and post-tensioning, both topics that were relevant for the numerical work. The theory is presented as Part I, while Part II is the submitted paper. The number of pages does not reflect the amount of work put into the respective parts. During this writing process, the vast majority of the time and effort have been put into the paper. This includes the tedious process of deleting, revising and rewriting, to meet the requirement of maximum 10 pages.

I would like to thank my supervisor, Jan Arve Øverli; first of all, for showing me confidence and making the bold proposal of writing a scientific paper; and secondly, for good guidance, willingly answering my questions and helping with the proofreading. I would also like thank Max Hendrix for help regarding the finite element program DIANA. Finally, I would like to thank Malin Anette Hallberg and Håvard Emaus Hanssen for providing all the data and calculations from the experiment.

Stine Maria Frøiland Jensen
Trondheim, December 2013

Abstract

This study consists of a numerical investigation of a post-tensioned flat slab without conventional longitudinal reinforcement; only steel fibres were employed to ensure sufficient ductility and shear capacity of the slab. Results were taken from a reported experiment conducted on a full scale steel fibre-reinforced flat slab (0.38% fibre content) which was tested until failure, undergoing a ductile bending failure at a load of 6.5 kN/m^2. A nonlinear finite element analysis was employed to study the experiment, including the ultimate state. A parametric study was performed using the numerical model to investigate the influence of the tensile behaviour of steel fibre-reinforced concrete (SFRC) on the response of the structure. The model proved to be relatively sensitive to changes in the tensile behaviour, but the differences were not prominent until entering the nonlinear area of the load-displacement curve. A constant curve with tensile stress equal to the residual tensile strength of the SFRC provided a robust numerical model and results on the conservative side. Including a peak stress with a multilinear tensile curve provided a less stable analysis but more accurate results. However, the model behaviour was stiffer than the experiment, providing too small deformations at failure. Nevertheless, the numerical model was able to display the ductile bending failure mode and moment redistribution.

Sammendrag

Denne studien består av en numerisk undersøkelse av et etterspent flatdekke uten vanlig lengdearmering; det ble kun brukt stålfiber for å oppnå tilstrekkelig duktilitet og skjærkapasitet i dekket. Resultatene er hentet fra et rapportert forsøk utført på et fullskala stålfiberarmert flatdekke (med fiberinnhold 0.38%), som ble lastet til brudd, hvilket resulterte i et duktilt momentbrudd ved en last på 6.5 kN/m^2. Forsøket har blitt modellert og analysert med ikke-lineær elementmetode, for å se på hele testforløpet, inkludert bruddgrensetilstanden. Den numeriske modellen ble benyttet til å gjennomføre en parameterstudie av egenskapene til stålfiberarmert betong i strekk, der det ble undersøkt hvordan disse egenskapene påvirket responsen til modellen. Den numeriske modellen viste seg å være relativt følsom overfor forandringer i strekkmodellen, men disse forskjellene ble ikke fremtredende før i det ikke-lineære området av last-forskyvningskurven. En konstant strekkmodell, med maksimal spenning lik reststrekkfastheten til den fiberarmerte betongen, viste seg å gi en robust numerisk modell og konservative resultater. Når strekkfastheten til betongen ble lagt inn ved hjelp av en multilineær strekkmodell, ble analysen mindre stabil, men resultatene mer nøyaktige. Modellen viste generelt en stivere oppførsel enn forsøket, og ga for små deformasjoner ved brudd. Den numeriske modellen var imidlertid i stand til å simulere det duktile momentbruddet og momentomfordeling i dekket.

Contents

List of Figures

Part I
THEORY

1 Introduction

Concrete is one of the most common building materials in civil engineering, due to its simple production, high compressive strength and versatility in form and application. However, concrete is a brittle material with a relatively low tensile strength, making it subjected to cracking. These problems are generally overcome by using reinforcement of various types; the most common is using regular reinforcement bars to carry tensile stresses where it is needed. Research has shown that labour on the construction site, such as preparation of formwork, placing of reinforcement bars and finishing of the concrete, can provide costs of the same magnitude as the material costs. Therefore, it is desirable to investigate new technologies that can contribute to saving labour time during construction and provide a more efficient solution.

Fibre-reinforced concrete (FRC) has many advantages; reduced crack widths and crack controlling, reduced steel reinforcement requirements, improved ductility and in some cases improved structural strength. In structural elements such as foundations, slabs-on-ground and walls, fibre can completely replace ordinary reinforcement. In load carrying elements such as beams and suspended slabs, fibre can be used in combination with regular or pre-stressed reinforcement. The fibre primarily improves the structural properties of the concrete by its ability to bridge cracks. In addition, the use of fibre reinforcement can save costs and valuable labour time during construction. Therefore, FRC is a material technology with great potential.

Post-tensioning of concrete is a well developed and common technology, which has proved to be a good solution regarding the brittleness and low tensile strength of the concrete. Benefits of post-tensioning include smaller crack widths and increased crack control, smaller deflections and more slender structures. Post-tensioning of flat slabs allows for smaller slab thickness and larger spans, which is desirable in many typical flat slab structures such as industrial buildings and parking garages.

In this part, background information and basic theory of fibre reinforced concrete and post-tensioning is presented. The aim of this part is to provide a general theoretical basis for the numerical investigation performed in Part II, and it covers mostly topics that have been relevant for the numerical work.

2 Fibre-reinforced Concrete

The material properties of concrete are characterised by a high compressive strength but a relatively low tensile strength and brittleness in tension, resulting in poor resistance to crack propagation. Including steel fibres or other dispersed fibrous reinforcement in the concrete can improve the mechanical properties of the concrete significantly. The main purpose of the fibre is to transfer tensile stresses across the cracks, through its ability to bridge cracks. This leads to better crack control and smaller crack widths, in addition to increased flexural stiffness, which are desirable properties in the service limit state [15]. Regarding the ultimate limit state, the fibre improves the properties of the concrete by providing larger ductility, toughness (residual load carrying capacity) and shear resistance [9].

In addition to improving the mechanical properties of the concrete, an important benefit of fibre is reduced building costs [14]. Use of fibre-reinforcement to replace mild reinforcement can save valuable labour time during construction. Research has shown that costs related to labour on the construction site, such as preparation of formwork, reinforcing, casting and finishing of the concrete, are almost as large as the material costs [15]. Fibre reinforcement is generally mixed into the concrete before pumping it into the formwork and thus no placement of reinforcement bars is necessary. Consequently, FRC contributes to reduced costs in construction work as well as simpler and faster construction.

2.1 Background and Current Status

The use of dispersed fibres in cement-based materials goes back to ancient times (approximately 3500 years ago) when sun-baked clay bricks were reinforced with straw or horse-hair. The concept of using steel fibres as reinforcement in concrete was proposed for the first time in the 1960s and has since evolved during the past 50 years [5].

FRC has long been a promising material. However, in Norway, until today the applications have mostly been limited to shotcrete and slabs-on-ground. Furthermore, the use of fibre has generally been for non-structural purposes, to control plastic and drying shrinkage [8]. The use of FRC in load carrying structures has been prevented due to lack of regulations and universally accepted calculation methods, which can be explained by some of the main challenges of FRC [12]:

1. Large variation in the residual tensile strength of FRC structures compared to standard test beams
2. Uncertainty related to toughness and ductility of FRC structures
3. Lack of appropriate methods for verification and control of cast structures

One of the most critical points in FRC theory is to predict the tensile behaviour of a structure and quantify the residual tensile stresses in a cracked section [9].

During the last decade, however, considerable research has been done on FRC, both nationally and internationally. There is an ongoing research project on fibre-reinforced concrete under the auspices of COIN (Concrete Innovation Centre), where one of the goals is to make the use of FRC in load carrying structures possible. Numerous experiments have been conducted, both laboratory tests and full scale field tests (see for instance [8] and [16]), largely focusing on the contribution of fibre in load carrying concrete structures, and gaining relatively good results. Also, steel fibre-reinforced concrete (SFRC) has been successfully employed in pre-stressed concrete bridge beams with no mild reinforcement [5], which shows that there is potential in using steel fibres in post-tensioned structures. One important observation from the conducted tests is that the residual tensile strength of FRC varies considerably from small test beams to full scale structures, by factors ranging from 0.4 to 2.0. The reason for this is not yet understood and represents a major obstacle in making regulations for fibre-reinforced concrete [14]. In Norway, a set of preliminary guidelines for structural design, application and control of FRC has been been established through the initiative of COIN [13]. However, fibre reinforcement is not yet included in Eurocode 2, and there is in general shortage of standardised calculation and strength verification methods for FRC [5].

2.2 Fibre Technology

Fibre-reinforced concrete contains dispersed, discontinuous discrete fibres that are distributed throughout the entire cross-section, unlike regular reinforcement which is only placed where it is needed. The main task of the added fibre is to bridge cracks that occur in the matrix and transfer tensile stresses across the cracks. The fibre contributes to improved crack control by causing large single cracks to be replaced by a system of microcracks with considerably smaller crack widths [5]. The effect of fibre in terms of crack bridging under the application of sectional forces M, V and N is illustrated and summarised in figure 1. As the figure shows, the fibre contributes in both compressive and tensile cracks, as well as shear-induced cracks.

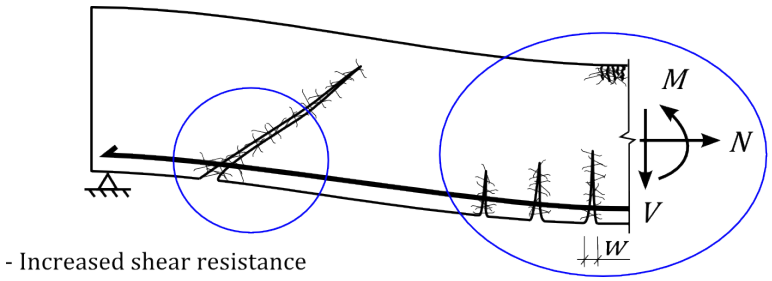

- Increased shear resistance
- Increased punching resistance
- Increased dowel effect
- Inhibits growth of splitting cracks
- Increased confinement of anchored bars

- Reduced crack spacing
- Reduced crack widths
- Increased moment resistance
- Increased flexural stiffness
- Increased ductility in compression

Figure 1: Effects of fibre on the structural behaviour [15]

Figure 2: Fracture surface of steel fibre-reinforced concrete [10]

For low to moderate fibre contents ($\leq 1\%$), the fibre benefits do not arise until after crack initiation and the the tensile strength of the composite material is not notably affected. The post-cracking behaviour of concrete, however, is significantly improved due to the fibre contribution. FRC obtains a significant increase in the ultimate tensile strain and displays a distinct and stable residual tensile strength after cracking, even as the crack widths increase [15].

Factors that influence the material properties of fibre-reinforced concrete are the individual material properties of the matrix and the fibres, respectively, and the bond strength between the matrix and fibres. Furthermore, the orientation and distribution of fibres within the matrix and the amount of fibres are of importance [4]. The fibre contribution leads to a more ductile failure for FRC than for plain concrete, and the failure is mainly caused by fibre pull-out [15]. Figure 2 shows a fracture surface of SFRC after failure due to fibre pull-out, in which the randomly distributed and oriented fibres are clearly displayed.

Failure of FRC due to fibre pull-out is desirable in order to obtain ductility and toughness during failure. Therefore, the fibre must be adequately ductile to prevent fibre fracture due to bending. Furthermore, the bond strength between the fibre and the matrix must be of the same magnitude, or higher, than the tensile strength of the matrix. For steel fibres with hooked ends a significant energy dissipation arises as the fibre is straightened and plastically deformed. This dissipated energy becomes part of the fracture energy of the concrete. The fracture energy (also called the toughness of the concrete) is defined as the area under the stress-crack opening ($\sigma - w$) – curve in tension and is the energy required for crack propagation [15]. Consequently, FRC displays significantly higher fracture energy than plain concrete.

Some basic requirements of the fibre are summarized in the following [15]:

- The fibre must have a tensile strength that is at least 2-3 times higher than that of the matrix
- The elastic modulus of the fibre must be at least three times as high as the one of the matrix

- The Poisson's ratio and thermal expansion coefficient of the fibre and the matrix must be of the same order of magnitude

2.3 Fibre Types

There are a number of different parameters that affect the properties and behaviour of fibre-reinforced concrete, including the properties of the actual fibres and the interaction between the fibre and the surrounding matrix. Numerous fibre types are available, of various materials, shapes and sizes, and they vary considerably in properties and effectiveness. Each fibre type is designed for a specific purpose, for instance to improve structural strength, to control drying shrinkage or to increase fire resistance of the concrete. The main types of fibre reinforcement used for structural purposes are [13]:

- Steel fibres
- Glass fibres
- Synthetic fibres
- Natural fibres

The size of the fibres varies, from lengths of a few millimetres (microfibres) to 80 mm (macro-fibres) and diameters from a fraction of a micrometer to 2 mm. There is also variety in the design of steel fibres, in terms of shape, cross-section and surface. The fibres can be straight, wave shaped, bow shaped, toothed, surface intended, twisted or irregular, as illustrated in figure 3. Anchorage of the fibre can be provided by hooked ends, paddles, end knobs or coned ends. The fibre cross-section can also differ, and available cross-sectional geometries include circular, rectangular, triangular and irregular cross-sections. The purpose of the design is to provide anchorage of the fibres and to gain sufficient bond between the fibre and the matrix [15]. For structural purposes, cold-drawn steel wire fibres are the most common. [13]. In this study, steel fibres have been employed, thus the properties described in the following are mainly related to SFRC.

2.4 Mechanical Properties

Concrete is generally classified by its compressive strength and this property constitutes the basis for design rules and defining concrete quality. When analysing fibre-reinforced concrete, however, one needs additional material parameters to describe the toughness and ductility provided by the fibre [15]. The basic design and classification parameter for fibre-reinforced concrete is the residual tensile strength, which characterises the ability to resist tensile stresses in a cracked section [13].

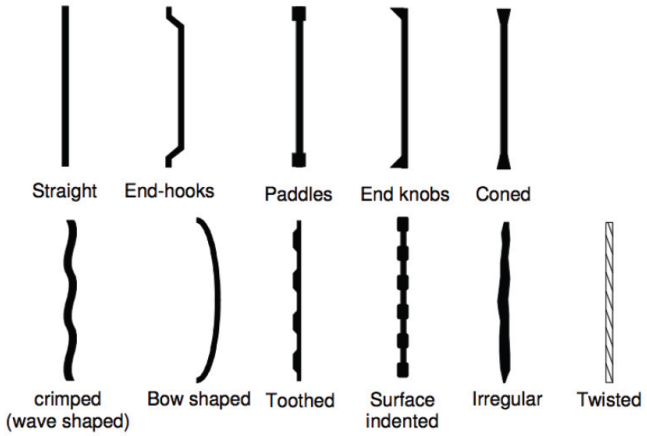

Figure 3: Different fibre geometries [15]

2.4.1 Compressive Properties

In compression, plain concrete behaves elastically until it reaches about 30% of the compressive strength, then it experiences gradual softening as the stress reaches the compressive strength. After the peak stress, strain softening occurs and eventually failure by crushing. Even though crushing is characterised as a compression failure, a uniaxial compression state failure is actually caused by tensile cracks. Tensile strains in the transverse direction cause minor cracks in the load direction (or the principal stress direction), and this is what causes crushing of the concrete [15]. The compressive behaviour of plain concrete and FRC is illustrated in figure 4.

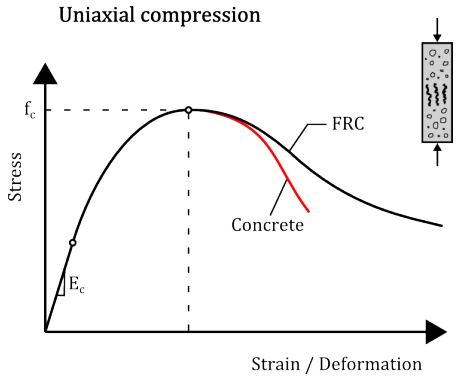

Figure 4: FRC in uniaxial compression [15]

Adding fibre to the concrete will contribute to crack control, as the main effect of the fibre is increased resistance against longitudinal crack growth. In general, when using a fibre content of less than 1.0%, conventional steel fibres do not affect the pre-peak properties in compression. This means that the compressive strength, the modulus of elasticity, Poisson's ratio and the thermal expansion coefficient remain the same as for

plain concrete. However, both the strain at crack localisation and the failure strain increase [15].

2.4.2 Tensile Properties

One of the most critical points in FRC theory is to predict the tensile behaviour of the material and especially to quantify the residual stresses in tension for a cracked section [9]. After cracking, the FRC displays a relatively stable residual tensile strength, even as the crack widths increase. The residual tensile strength, $f_{t,res}$, is defined as the residual tensile force resultant acting on a unit area of a cracked section in the concrete [13]. For modelling the tensile behaviour of FRC, the contribution of fibres can be introduced by considering FRC as a homogeneous material with higher toughness, represented by the residual tensile strength.

Classification of tensile behaviour of FRC is based on uniaxial tension response which can be either strain-softening (quasi-brittle) or pseudo strain-hardening. The former is the case for regular FRC and plain concrete while the latter applies to high-performance FRC. Figure 5 shows a typical material curve for regular FRC and plain concrete under uniaxial tensile loading. For strain-softening materials a localised single crack characterises the tensile behaviour, as seen in the tensile diagram.

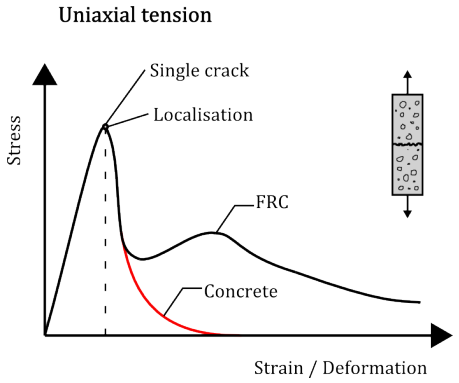

Figure 5: Tensile behaviour of FRC in uniaxial stress state [15]

In comparison to plain concrete, neither the tensile strength nor the modulus of elasticity of fibre-reinforced concrete is significantly affected. The fibre mainly affects the tensile fracture behaviour and the post-cracking properties. For FRC, the fracture energy and the shape of the stress-strain curve can vary greatly, depending on fibre type, amount of fibres and concrete quality, to name a few. For FRC with a low to moderate fibre content ($< 1\%$) the stress-strain curve is characterised by a strain-softening behaviour, as shown in figure 5. After the tensile strength is reached, the curve decreases relatively steeply, but whereas the curve for plain concrete continues decreasing until zero, the curve for FRC typically increases again as the fibre starts acting by carrying tensile stresses across cracks. The last part of the curve, having an approximately constant stress value, displays the residual tensile strength of the FRC.

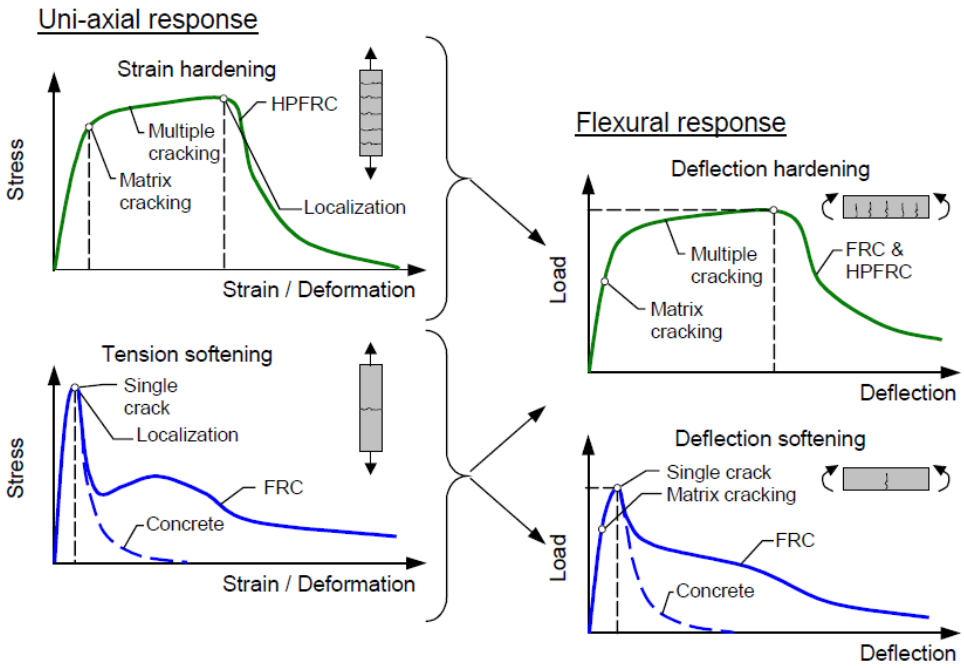

Figure 6: Typical tensile and flexural behaviour of FRC [15]

Figure 6 shows typical tensile and flexural behaviour of FRC. As seen in the figure, FRC can display relatively different tensile behaviour in uniaxial tension and in flexural tension, respectively. The figure shows the difference between hardening and softening behaviour, and shows that the tension softening behaviour is characterised by crack localisation, while for a hardening material, multiple cracking occurs. Also, the figure shows that even though the FRC displays softening behaviour in uniaxial tension, it may obtain multiple cracking and hardening in flexural bending.

2.4.3 Shear Properties

For plain concrete, the mechanisms leading to transferring of shear stresses across cracks include aggregate interlocking and friction at crack faces. For FRC, the fibre is activated after cracking and failure eventually occurs due to fibre pull-out, leading to a significantly toughening behaviour. It has been shown that by adding fibre to the concrete the shear transfer capacity can be increased to as much as 60% of the compressive strength. Further, the shear strength increases with the fibre volume fraction [15].

2.4.4 Design and Classification of FRC

The post-cracking properties of FRC, namely its ductility and toughness, are commonly quantified by the residual tensile strength of the FRC. The preliminary guidelines specify the characteristic residual tensile strength at a crack width of 2.5 mm, $f_{ftk,res,2.5}$,

to be used for classification of FRC [13]. This parameter also constitutes the basis for design in both service and ultimate limit states. Further, the preliminary guidelines distinguish between the residual tensile strength and the residual flexural tensile strength of FRC. The relation between the flexural tensile strength at a 2.5 mm crack width, $f_{Rk,3}$, and the residual tensile strength is given as:

$$f_{ftk,res,2.5} = 0.37 f_{Rk,3} \tag{2.1}$$

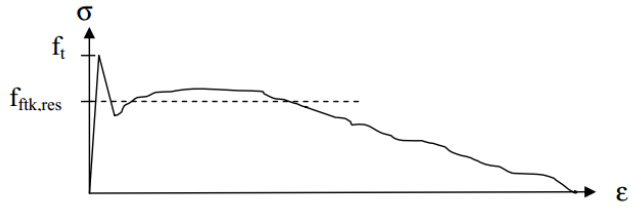

Figure 7: Residual tensile strength of FRC [8]

The flexural residual tensile strength is determined from bending tests of standard test beams. The tests must be performed in accordance with recognised standard test methods approved by [13]. Two of these methods are the 3-point bending test for standard notched beams according to NS-EN 14651 [6] and the 4-point bending test for unnotched sawn beams, the Norwegian Standard Bending Test (NSBT), according to a previous set of guidelines made for the Norwegian Concrete Association in 2006 [19]. From the standard bending tests, the bending moment at a 2.5 mm crack width is found, from which the flexural residual tensile strength, $f_{Rk,3}$, can be taken. Then equation (2.1) is employed to calculate $f_{ftk,res,2.5}$. Figure 7 shows a typical response curve from a bending test, displaying a peak stress equal to the tensile strength of the concrete and a residual tensile strength after crack propagation. As of today, the residual tensile strength of FRC must be determined through testing. For FRC structures, test beams from the FRC can be cast and tested to find the correct material properties.

The preliminary guidelines define three decisive characteristics of FRC; the mechanical strength, fibre distribution and fibre orientation [13]. If the fibre distribution or orientation in the structure is different from the test beams, the residual tensile strength of the structure can be found with the use of a fibre orientation factor or by including the fibre content in the calculations [13].

2.4.5 Fibre Orientation and Distribution

The fibre content (volume fraction) is of large significance for the material behaviour and strength of FRC. Other important parameters are the distribution and orientation of the fibre in the matrix. These parameters are difficult to predict as they may vary from one structure to another, or within a structure. Local effects and obstacles, such

as reinforcement bars, may cause fibre concentrations and uneven fibre distribution in a structure, which is unfavourable [13].

The fibre is generally mixed into the concrete before pumping the concrete into the formwork, and the aim is to obtain a random fibre distribution and orientation. The distribution and the orientation of the fibre can be influenced by factors such as method of placement, equipment used and properties of the fresh concrete.The geometry of the cast cross-section also affects the fibre distribution and orientation, as the fibre may be prevented from distributing freely [15].

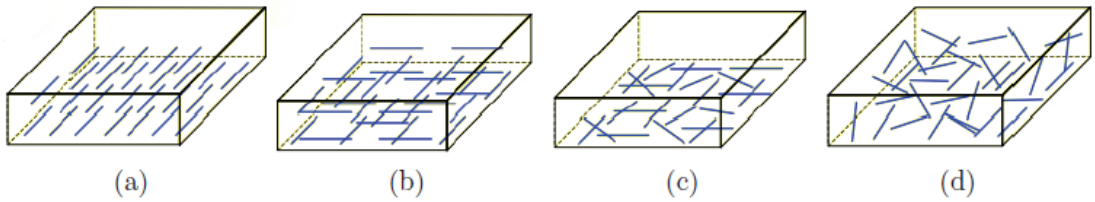

Figure 8: Various fibre distributions: (a) direct 1-D fibre orientation, (b) direct 2-D fibre orientation, (c) plane-random fibre orientation, and (d) body-random fibre orientation [15]

Fibre orientation and distribution can be either direct or random (free), in 1, 2 or 3 dimensions, respectively. If one dimension of the structural element, for instance the plate thickness, is smaller than the length of the fibre, the fibre will obtain a plane-random orientation with a free distribution of fibres in two dimensions only. With all dimensions considerably larger than the fibre length, the fibre will obtain a body-random orientation and distribute freely throughout the structural element, in all 3 directions. The various cases are illustrated in figure 8.

The material properties of FRC depend on the fibre content and the distribution and orientation of the fibre in the concrete. This can be accounted for by introducing the fibre orientation factor, which defines the efficiency of bridging in terms of amount of fibres bridging a crack and fibre orientation effects. As presented in section 2.4.4, this factor can be included in the calculation of the residual tensile strength to account for differences in fibre distribution or orientation between test specimens and the structure. In general, the fibre efficiency increases for smaller dimensions and for more homogeneous fibre distribution [15].

2.5 Concluding Remarks

Describing the behaviour of fibre-reinforced concrete is far from straight forward as the behaviour and characteristics of the material depend on numerous factors. For instance, the fibre volume fraction is of large significance for the influence of the fibre on the structural properties of the FRC. For low to moderate fibre contents (less than 1.0%) the fibres have negligible effect on the strength, both in tension and compression. The main

effect of the fibre is to improve post-cracking behaviour and toughness of the concrete by allowing for tensile strains at rupture, thus causing increased capacity of transferring stresses after matrix cracking. This effect is quantified by the residual tensile strength of the FRC, which is displayed as a constant residual stress after crack propagation in the tensile stress-strain diagram of FRC. The residual tensile strength constitutes the basis for design and classification of FRC. The contribution of the fibre can therefore significantly improve the mechanical properties of the concrete, by providing ductility, shear resistance and larger ultimate load capacity. However, due to lack of regulations and universally approved calculation and verification methods, the use of fibre reinforcement in load-carrying concrete structures is limited.

3 Post-tensioning

Pre-stressing the concrete by using post-tensioned reinforcement provides less cracking and smaller crack widths, causing better durability of concrete structures and preventing corrosion problems. Furthermore, pre-stressing leads to smaller deflections and allows for more slender structures and smaller overall construction heights. The concrete is pre-stressed by inserting post-tensioning reinforcement, which applies compressive stresses to the concrete. The compressive stresses are applied with a beneficial size and distribution in order to balance the effects of the external loads. Post-tensioned flat slabs are commonly used in industrial buildings, parking garages and other structures where large open areas are required. In comparison to normal reinforced concrete, post-tensioning allows for reduced slab thickness and larger spans.

3.1 Principle of Pre-stressed Concrete

Regular or mild reinforcement is added to concrete to provide tensile strength and limit crack widths. Regular reinforcement can be called a passive reinforcement because it does not carry loads until the concrete has started cracking. Post-tensioning, however, provides an active reinforcement. The pre-stressing reinforcement applies compression to the concrete in those regions that will be subjected to tensile stresses during loading. These compressive stresses will offset the tensile stresses produced by the loads [2]. Figure 9 illustrates the principle of post-tensioned reinforcement and shows regular reinforced concrete that cracks under loading, post-tensioned concrete before loading and post-tensioned concrete after loading.

Thus, the total tensile stresses in the concrete will be significantly reduced, as will the crack propagation and crack widths. The deflections will also be reduced because the post-tensioning compressive stresses cause a negative deflection that will be balanced by the deflections induced by the self-weight and exterior loads [2].

3.2 Applications and Benefits

The use of pre-stressed concrete or post-tensioning provides many advantages compared to regular reinforcement. Firstly, post-tensioning leads to less cracking and smaller crack widths, causing better durability of the structure and preventing corrosion problems. This also assures waterproof structures. The overall flexural stiffness is increased and constructing stiff corners and connections becomes easier. For slabs, the slab thickness can be reduced by as much as 30%. This produces less dead weight and less loading on internal walls, columns and foundations, in addition to reduced material use and reduced overall height. The total amount of reinforcement is also reduced, as less steel is required for post-tensioning, compared to regular reinforcement. Hence, post-tensioning is both time- and cost-saving as less reinforcement needs to be placed and

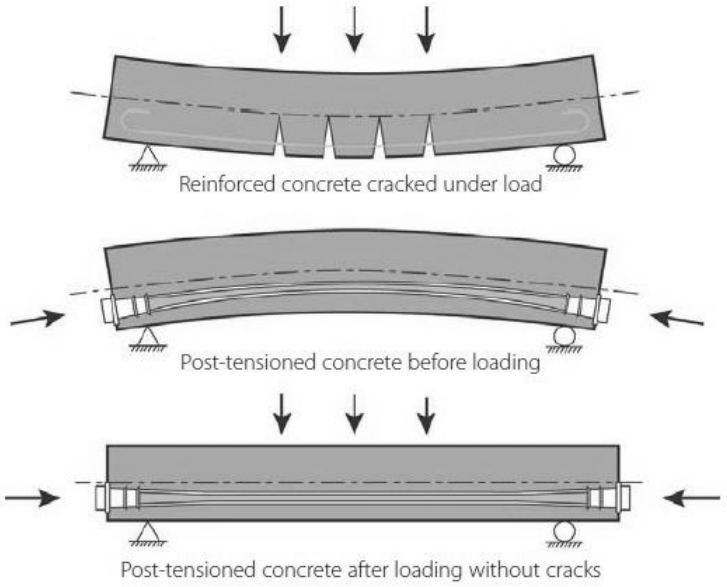

Figure 9: Principle of post-tensioned reinforcement [2]

less material is required. Post-tensioning also contributes to significantly smaller and better controlled deflections which allows larger spans and more slender structures. In general, post-tensioning provides larger freedom when designing structures [18].

Application of post-tensioning systems has a wide range and the technology is being used in various structures such as bridges, buildings, dams, marine structures and tunnels [2].

Post-tensioning is frequently applied in typical flat slab structures where large spans are required. Examples of such structures are industrial buildings, parking garages, warehouses, office buildings, schools and apartment buildings. A single tendon system is commonly employed for flat slabs with relatively small slab thicknesses. Its most common application is in parking garages with spans of 16-17 meters, but it may constitute an economically favourable option even for spans down to 6 meters [18].

3.3 Single Strand Tendons

Single strand tendon technology, which has been used in the experiment of this study, consists of single tendons that are tensioned separately. Figure 10 shows the single strand tendon system in a flat slab before casting.

One strand or tendon consists of seven wires made of high strength steel. During construction, the tendons are laid out with the correct profiles and spacing after the formwork has been installed, before the concrete is cast. When the concrete has reached its minimum strength, the tendons can be stressed using a hydraulic jack, and anchored at

Figure 10: Tendons laid out in a flat slab structure [18]

the ends. The pre-stressing force is applied to the tendon at the anchorage and transferred to the surrounding concrete. The tendons have one anchor in each end, either one active and one passive, or two active anchors [2].

3.4 Bonded vs. Unbonded Tendons

In bonded systems the tendons are fully bonded to the surrounding material. The tendons are inserted into ducts and after the pre-stressing load is applied, the ducts are filled with cementitious grout to provide bond between the tendon and the concrete [3]. This is shown in figure 11(a). For bonded systems, there is in principle uniform steel-concrete force transfer along the length of the tendons and full strain compatibility is assumed, implying that steel strains are equal to the concrete strains. Cracks are restrained locally by the steel being bonded to the adjacent concrete. Furthermore, if a tendon is locally damaged, the concrete will retain its pre-stressing due to the steel-concrete bond [11].

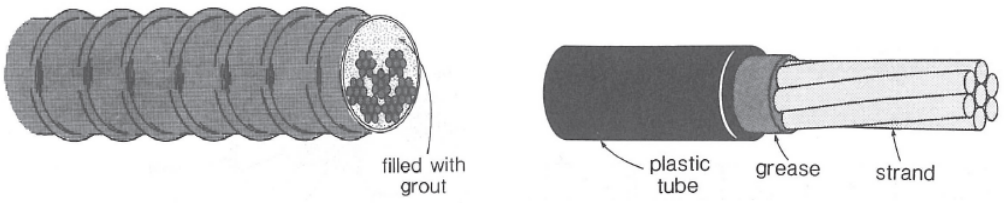

(a) Grouted and bonded multi-strand tendon in duct

(b) Plastic sheathed unbonded monostrand tendon

Figure 11: Principle of bonded and unbonded tendons [7]

For unbonded tendons, each tendon is greased and covered by a plastic tube, as shown in figure 11(b), to avoid corrosion and to provide minimum friction between the tendon and the concrete [18]. This solution is advantageous because it allows de-stressing before attempting repair work and there is no need for grouting, which can be an intricate procedure. However, if the tendon is damaged, it will lose all of its pre-stressing at once [3]. For unbonded tendons, steel-concrete force transfer occurs only at the anchors and

strain compatibility cannot be assumed at all sections. Cracks are restrained globally due to the strain in the tendon but large cracks may occur. It is recommended that an additional minimum amount of mild reinforcement is provided when using unbonded tendons to prevent large cracks [11].

3.5 Pre-tensioning vs. Post-tensioning

Pre-stressed concrete can be achieved either by pre-tensioning or post-tensioning of the reinforcement. Pre-tensioned systems are primarily used for pre-fabricated concrete elements and the elements are produced in a precast plant. Further, the system is limited to straight, harped or circular tendons [3]. Pre-tensioning is in general carried out by inserting the tendons into a preformed casting bed and applying the pre-stressing force before the concrete is cast. When the concrete is hardened, the tendons are cut and the pre-stress is transferred to the concrete from the anchorages due to bond between the tendons and the concrete [17].

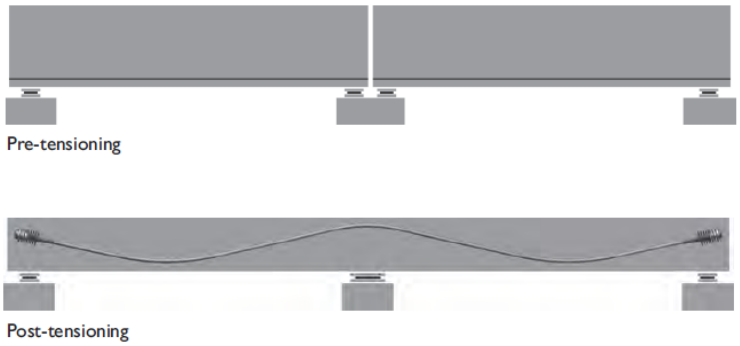

Figure 12: Pre-tensioning vs. post-tensioning [3]

Post-tensioned systems are usually made on site and allow almost any shape of the tendons, and they can be made to meet nearly any design requirement. The tendons can be bonded or unbonded, and internal or external [3]. The procedure for casting post-tensioned concrete is described in section 3.3.

3.6 Material Properties

In order to provide full pre-stressing of concrete during a the service life of a structure, the tendons must be made from high strength steel. Over time the pre-stressing force in the tendons will be reduced due to effects such as creep, shrinkage or relaxation of the steel. The initial pre-stressing force must therefore be large enough to ensure sufficient post-tensioning after losses and thus keep the concrete in full pre-stressing. If regular reinforcement steel was to be used, the dimensions would have to be correspondingly larger and one would lose some of the benefits of post-tensioning. Also, since regular

and high strength steel have approximately the same elastic modulus, high strength steel will suffer from smaller pre-stress losses in percentage [17].

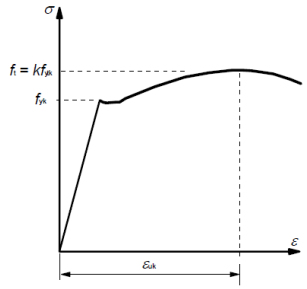

(a) Regular reinforcement steel

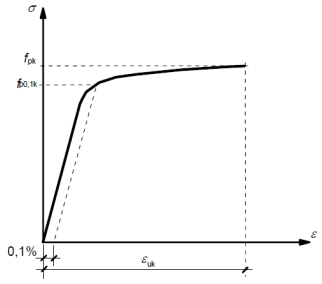

(b) Cold drawn high strength steel

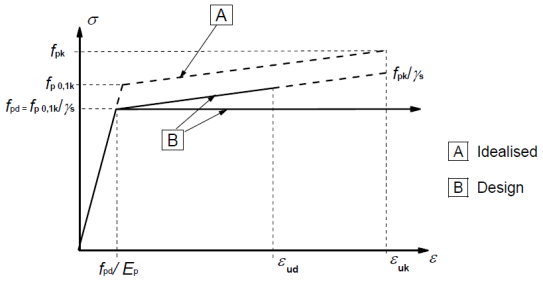

(c) Idealised and design diagram for pre-stressing steel

Figure 13: Some $\sigma - \varepsilon$-relations for reinforcement steel [1]

High strength steel is made by a combination of alloying and cold drawing. It does not have a distinct yield limit such as regular reinforcement steel, as seen in the stress-strain diagrams in figures 13 (a) and (b). Therefore, in Eurocode 2 the characteristic strength of the material is defined as the "0.1%-limit", $f_{p0.1k}$, which is the stress value corresponding to an inelastic strain of 0.1% [17].

3.7 Equivalent Loads

The aim of the post-tensioned reinforcement is to balance the effect of external loads. For beams or slabs subjected to uniformly distributed load, the resulting bending moment distribution will have the shape of a parabola and the tendons should be curved in the same shape in order to balance the load-induced stresses. Therefore, placing tendons in a parabolic shape according to the distribution of external moments is common practice.

For a parabolic-shaped tendon the pre-stressing force will try to straighten it out, but the tendon is restrained from moving by the surrounding concrete. This will cause transverse forces to act from the tendon to the concrete, as illustrated in figure 14. These

transverse forces are defined as equivalent loads and denoted p.

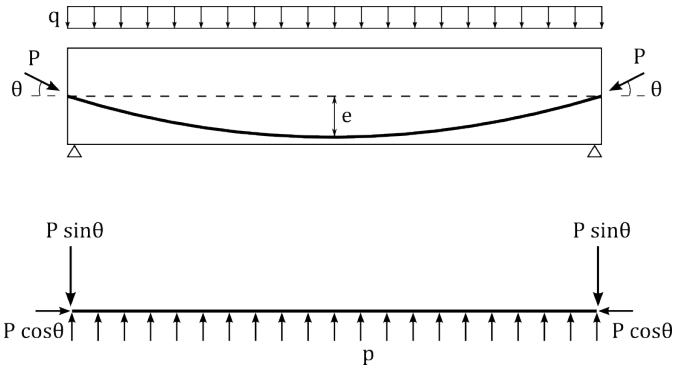

Figure 14: Equivalent loads due to post-tensioning force P

Depending on the aim of the design, the post-tensioning can be conducted to fully balance both dead weight and external loads, the dead weight and portions of the external loads or only the dead load, respectively.

3.8 Loss of Pre-stress

Loss of pre-stress in tendons occurs due to various reasons such as relaxation of the steel (viscoelastic extension), creep (viscoelastic shortening) and shrinkage (shortening due to initial strain) of the concrete, friction between the tendon and the surrounding material or penetration of the anchorage. Because of the losses, the force in the tendons decreases as the distance to the anchorage increases [20].

Friction losses occur due to friction between the tendon and the surrounding material. The friction consists of two parts; the contribution from the curvature of the tendon, and the friction due to local irregularities (wobble) [20].

For a curved tendon the pre-stressing force P causes a pressure p on the concrete due to the curvature of the tendon (see figure 14). The reduction of the pre-stressing force due to the pressure p can be determined as the friction coefficient μ times the transverse force p [20] :

$$\Delta P = \mu p \tag{3.1}$$

μ is defined as the Coulomb friction coefficient between the tendons and the sheathing. For normal unbonded single tendons with greasing and plastic sheathing the friction coefficient is in the order of magnitude $\mu = 0.05 - 0.07$ [17].

The wobble effect is the pre-stressing friction loss caused by local irregularities along the tendon. Even a straight tendon will never be perfectly straight and this effect is included by introducing the wobble parameter.

Long-time effects such as creep, shrinkage and relaxation are not regarded in this study.

3.9 Concluding Remarks

Post-tensioning of concrete provides smaller crack widths and better crack control, smaller deflections and more slender structures. The technology is commonly used for a vast array of structures, and it allows for larger freedom when designing structures. The stresses in the concrete due to external loads are balanced by equivalent loads applied by the post-tensioning. Placing the tendons with a curved profile provides beneficial pre-stressing for evenly distributed loads. Single strand tendons are commonly used in flat slabs, providing smaller deflections during loading and allowing smaller slab thickness and larger spans.

References

[1] Eurocode 2: Design of concrete structures: Part 1-1: General rules and rules for buildings. NS-EN 1992-1-1:2004+NA:2008, 2008.

[2] VT International Ltd BBR. Post-tensioning - where creativity meets strength. http://www.bbrnetwork.com/downloads/brochures.html, http://www.bbrnetwork.com/downloads/brochures.html, 2008.

[3] VT International Ltd BBR. CONA CMX Volume 1 - system applications. http://www.bbrnetwork.com/downloads/brochures.html, September 2013. Strand Post-tensioning Systems.

[4] Arnon Bentur and Sidney Mindess. *Fibre reinforced cementitious composites*. Taylor & Francis, 2006.

[5] Andrzej M Brandt. Fibre reinforced cement-based (FRC) composites after over 40 years of development in building and civil engineering. *Composite Structures*, 86(1):3–9, 2008.

[6] European Committee for Standardization CEN. Test method for metallic fibre concrete. Measuring the flexural tensile strength (limit of proportionality (LOP), residual), NS-EN 14651:2005+A1:2007, 2007.

[7] Michael P Collins and Denis Mitchell. *Prestressed concrete structures*, volume 9. Prentice Hall Englewood Cliffs, 1991.

[8] Åse Døssland. *Fibre reinforcement in load carrying concrete structures*. PhD thesis, Norwegian University of Science and Technology, 2008.

[9] Viktor Gribniak, Gintaris Kaklauskas, Albert Kwok Hung Kwan, Darius Bacinskas, and Darius Ulbinas. Deriving stress–strain relationships for steel fibre concrete in tension from tests of beams with ordinary reinforcement. *Engineering Structures*, 42:387–395, 2012.

[10] Malin Anette Hallberg and Håvard Emaus Hanssen. Post-tensioned fibre reinforced flatslab. Master's thesis, Norwegian University of Science and Technology, 2013.

[11] Trey Hamilton. Design of post-tensioned components for flexure, section 3. http://www.post-tensioning.org/Uploads/EducationOctober 2013.

[12] Terje Kanstad, Malin Anette Hallberg, Håvard Emaus Hanssen, and Steinar Trygstad. Rik på fiber. In *Rapport - Betonginformasjonsdag 2013*, October 2013.

[13] Terje Kanstad, Dan Arve Juvik, Arne Vatnar, Alf Egil Mathisen, Sindre Sandbakk, Hedda Vikan, Eirik Nikolaisen, Åse Døssland, Nils Leirud, and Geir Ove Overrein. Forslag til retningslinjer for dimensjonering, utførelse og kontroll av fiberarmerte betongkonstruksjoner. In *COIN Project report no 29*. SINTEF Building and Infrastructure, COIN, 2011.

[14] Terje Kanstad, Sindre Sandbakk, Mette R. Geiker, and Tor Arne Martius-Hammer. Flowable fibre reinforced concrete: Materials development, fibre distribution and structural properties. *Concrete Under the Northern Lights*, -:60–65, 2013.

[15] Ingemar Löfgren. *Fibre-reinforced concrete for industrial construction-a fracture mechanics approach to material testing and structural analysis*. PhD thesis, Chalmers University of Technology, 2005.

[16] Sindre Sandbakk. *Fibre Reinforced Concrete: Evaluation of test methods and material development*. PhD thesis, Norwegian University of Science and Technology, 2011.

[17] Svein Ivar Sørensen. *Betongkonstruksjoner - Beregning og dimensjonering etter Eurocode 2*. Tapir Akademisk Forlag, 2009.

[18] Spennteknikk. BBR VT CONA Single spenntausystem. http://www.spennteknikk.no/brosjyrer/BBR-VT-CONA-Single-spenntausystem-24022011.pdf, February 2011.

[19] Erik Thorenfeldt, S Fjeld, et al. Stålfiberarmering i betong. Veiledning for prosjektering, utførelse og kontroll. *Høringsutkast Mai*, 2006.

[20] TNO. *Diana User's Manual*. TNO DIANA, January 2012. Diana version 9.4.4.

Part II
PAPER

Numerical Investigation of a Post-tensioned Flat Slab with Steel Fibre Reinforcement

Stine Maria Frøiland Jensen and Jan Arve Øverli
Department of Structural Engineering
Norwegian University of Science and Technology
7491 Trondheim
E-mail: stinemje@stud.ntnu.no

Abstract

This paper presents a numerical investigation of a post-tensioned flat slab without conventional longitudinal reinforcement; only steel fibres were employed to ensure sufficient ductility and shear capacity of the slab. Results were taken from a reported experiment conducted on a full scale steel fibre-reinforced flat slab (0.38% fibre content) which was tested until failure, undergoing a ductile bending failure at a load of 6.5 kN/m^2. A nonlinear finite element analysis was employed to study the experiment, including the ultimate state. A parametric study was performed using the numerical model to investigate the influence of the tensile behaviour of steel fibre-reinforced concrete (SFRC) on the structural response. The model proved to be relatively sensitive to changes in the tensile behaviour, but the differences were not prominent until entering the nonlinear area of the load-displacement curve. A constant curve with tensile stress equal to the residual tensile strength of the SFRC provided a robust numerical model and results on the conservative side. Including a peak stress with a multilinear tensile curve provided a less stable analysis but more accurate results. However, the model behaviour stiffer than the experiment, providing too small deformations at failure. Nevertheless, the numerical model was able to display the ductile bending failure mode and moment redistribution.

Keywords:
Steel fibre reinforcement, post-tensioning, flat slab, nonlinear finite element analysis

1 INTRODUCTION

Concrete is one of the most important building materials in civil engineering, due to its simple production, its high compressive strength and versatility in form and application. Some major disadvantages of concrete, however, are its brittleness and low tensile strength, resulting in poor resistance to crack propagation. Adding steel fibres to the concrete can provide a solution to these challenges and improve the mechanical properties of the concrete significantly. The main task of the fibres is to bridge cracks and transfer tensile stresses across cracks. This leads to better crack control and smaller crack widths, in addition to increased flexural stiffness, which

are desirable properties in the service limit state [1]. Regarding the ultimate limit state, the fibre provides larger ductility, toughness (residual load carrying capacity) and shear resistance [2]. In addition to improved mechanical properties, important benefits of steel-fibre reinforced concrete (SFRC) include efficiency and reduced costs during construction. Valuable labour-time can be saved by using SFRC as placement of reinforcement is not required, making SFRC an economically favourable and more efficient solution.

The tensile behaviour of SFRC is characterised by a distinct and stable residual tensile strength after cracking. According to preliminary guidelines to design of SFRC created by COIN (Concrete Innovation Centre) [3], the characteristic residual tensile stress taken at a crack width of 2.5 mm, $f_{ftk,res2.5}$, constitutes the basis for design in service and ultimate limit states. The residual tensile strength must as of today be determined through bending tests of standard test beams, as described in [3]. The residual tensile strength and other material properties of SFRC are dependent on the fibre content as well as the distribution and orientation of the fibre in the concrete. The fibre orientation factor defines the efficiency of bridging in terms of amount of fibres in a cracked section and fibre orientation effects. In general, the fibre orientation factor increases for smaller dimensions and for more homogeneous fibre distribution [1].

Until today the use of SFRC has mostly been limited to shotcrete and slabs-on-ground. Application in load carrying structures has been prevented due to lack of regulations, although considerable research has been done on the topic during the last decade [4]. Numerous experiments have been conducted, both laboratory tests and full scale field tests (see for instance [5] and [6]), largely focusing on fibre in load carrying concrete structures, gaining relatively good results. SFRC has also successfully been employed in post-tensioned structural elements with no mild reinforcement [7]. One important observation from these tests is that the residual tensile strength of SFRC varies considerably from small test beams to full scale structures. The reason for this is not yet understood and represents a major obstacle in making regulations for SFRC [8].

This study contains numerical investigations of a reported experiment conducted on a full scale SFRC flat slab, which was tested to failure. The slab was post-tensioned but had no conventional longitudinal reinforcement; only steel fibres were employed to ensure sufficient ductility and shear capacity. Nonlinear structural analyses have been performed with the finite element code DIANA [9]. The aim of the numerical investigations is to provide a verification of the executed experiment and to explore how SFRC is implemented in a finite element model. A parametric study has been conducted to obtain the optimal material parameters for modelling tensile behaviour of SFRC.

2 EXPERIMENTAL STUDY

The full scale SFRC flat slab was post-tensioned but contained no mild reinforcement. The slab was subjected to evenly distributed load until collapse occurred, to observe the contribution of fibre in the ultimate limit state. All results from the experiment and other relevant information

used in this study were taken from [10].

2.1 Geometry and test set-up

The slab measured 17.3 m x13.4 m and was 210 mm thick. It was supported by six columns and one wall, giving spans with effective lengths 8.5 m and 6.5 m, respectively. The full geometry of the slab is shown in Figure 1. The column cross-sections were 300 mm x 300 mm and the wall thickness was 200 mm. The SFRC used was a self-compacting concrete with fibre content of 30 kg/m^3 or 0.38 volume-% steel fibres of length 50 mm and diameter 0.8 mm and hooked ends from KrampeHarex [11]. The slab was post-tensioned in both directions with curved single strand tendons with diameter 16 mm, with distribution as shown in Figure 1. The concentrated tendons above the columns were placed in bundles of two and three, respectively. The curved tendon profiles are shown in Figure 2 for each direction. The tendons were unbonded, which was achieved by greasing and plastic sheathing to provide minimal friction. Three LVDT sensors were mounted to measure the deflections of the slab, in the positions shown in Figure 1. LVDT 1 and 2 were placed in the critical span where maximum deflection would occur according to static beam formulas; $3L/8$ from the edge of the slab. All measurements started at zero when the experiment started, thus only the response from the water load was measured.

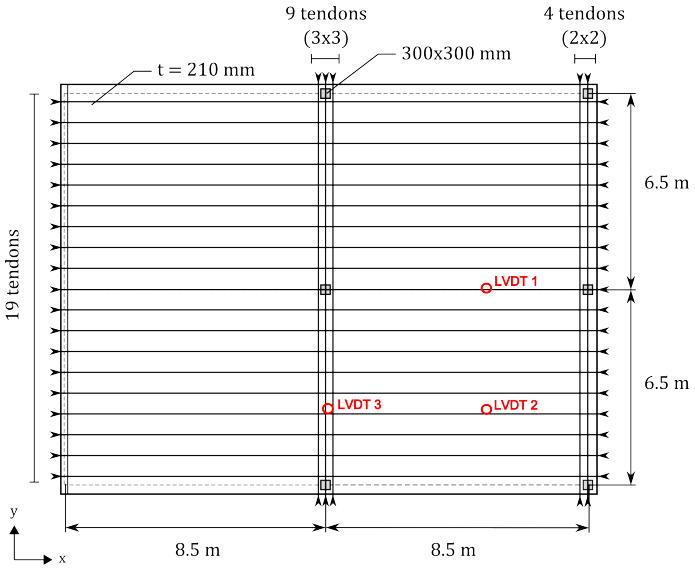

Figure 1: Geometry of test slab inlcluding LVDT positions

The slab was loaded with water to ensure an evenly distributed and steadily increasing load. The water was pumped into a formwork on top of the slab until collapse occurred, at a water load $q_w = 6.5$ kN/m^2. The dead weight of the slab of density $\rho_c = 24$ kN/m^3 was $g = 5.04$ kN/m^2. Each tendon was post-tensioned with a force of 220 kN 5 days after casting, and the post-tensioning force after losses was assumed to be 200.9 kN. The experiment was conducted after 29 days.

Failure occurred due to bending moment in the exterior span at a water height of 65 cm, at a

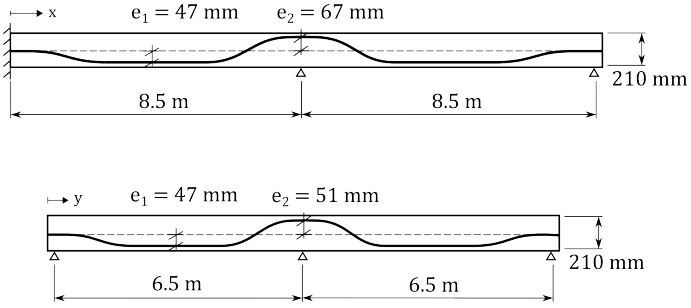

Figure 2: Tendon profiles in the longitudinal direction

failure load considerably higher than expected. The failure mode was a characteristic ductile failure with large deflections and rotations before collapse, see Figures 3 and 4, and it was predicted by [10] on the basis of yield line theory. The punching shear capacity proved to be sufficient, due to the contribution of the fibre. Further, the test results showed that significant moment redistribution occurred during the experiment, hence the SFRC had sufficient ductility for plastic deformation and moment distribution to occur.

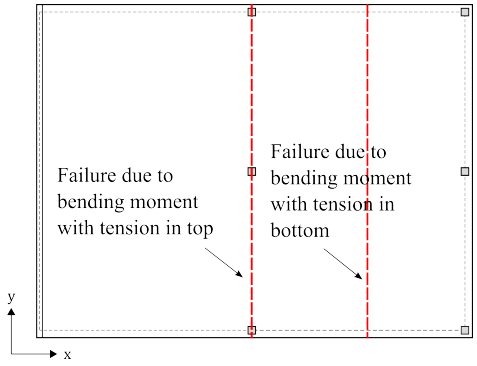

Figure 3: Failure mode of test slab showing the yieldlines

Figure 4: The test slab at the moment of collapse [12]

2.2 Material properties

Six cylinders and six standard beams were cast from the same SFRC batch as used in the slab and 15 standard beams were sawn from the slab after the experiment. The cylinders were tested in uniaxial compression tests which resulted in a characteristic compressive strength of $f_{ck} = 47.4$ MPa and a mean compressive strength of $f_{cm} = 49.3$ MPa. The standard beams were subjected to bending tests to determine the residual tensile strength of the SFRC, and both the characteristic values ($f_{ftk,res2.5}$) and the mean values ($f_{ftm,res2.5}$) were found. The six cast beams were subjected to 3-point bending tests for notched beams [3] while for the sawn beams from the slab a 4-point bending test was used [13], and calculations were done according to both [13] and [3]. The results from the bending tests are given in Table 1.

The fibre orientation factor was approximately the same for all the sawn beams from the slab.

Table 1: Residual tensile strength of SFRC, from bending tests

	$f_{ftk,res2.5}$ (MPa)	$f_{ftm,res2.5}$ (MPa)
3-point bending test [3]	0.97	1.54
4-point bending test [13]	0.45	1.10
4-point bending test, calculated after [3]	0.25	1.03

The cast test beams, however, displayed a significantly higher fibre orientation factor, presumably because the small dimensions of the formwork provided a more uniform fibre distribution in the cast beams. Therefore, the residual tensile strength from the sawn beams was considered more representative for the experiment, and was employed for the analyses in this study. The material properties of the concrete (taken from Eurocode 2 [14] on the basis of the obtained compressive strength) and the post-tensioning reinforcement are summarised in Table 2.

Table 2: Material properties of the concrete and tendons

Concrete			Tendons		
Compressive	f_{ck}	47.7 MPa	Yield strength	$f_{p0.1k}$	1670 MPa
strength	f_{cm}	49.3 MPa	Ultimate strength	f_{pk}	1860 MPa
Tensile strength	f_{ctm}	3.8 MPa	Net diameter	ϕ	16 mm
Density	ρ_c	24 kN/m^3	Cross section area	A_p	150 mm^2
Elastic modulus	E_c	36000 MPa	Elastic modulus	E_s	195000 MPa
Poisson's ratio	ν	0.2			

3 NUMERICAL MODEL

In this section, the numerical model of the flat slab is presented. The slab was modelled using the finite element code DIANA [9] which is based on the displacement-method and well developed for nonlinear analysis of reinforced concrete structures.

3.1 Material models

Concrete in compression is characterised by a nonlinear pressure-dependent behaviour. A total strain approach with a multilinear stress-strain curve given by Eurocode 2 [14] was used for the compressive behaviour, assuming no effect of lateral confinement and cracking. The low fibre content of 0.38% was assumed not to affect the properties in compression. The steel fibres were added by including the residual tensile strength in the constitutive model in tension. Constant and multilinear tensile models were employed, and a parametric study was performed to find the optimal tensile properties. Furthermore, a smeared crack approach was employed in combination with a total strain rotating crack model. This crack model allows cracks to rotate as the principal strain direction changes [9]. The post-tensioning reinforcement was modelled as elastic-perfectly plastic and the yield limit was set to be the ultimate strength of the steel, $f_{pk} = 1860$ MPa.

3.2 Finite element model

Due to symmetry, only half of the slab was modelled. The slab model measured 17 m x 6.5 m and included only the effective spans. The columns were modelled as point supports and restrained against vertical displacement while the connection to the wall was assumed to be fixed. To avoid numerical problems and large stress concentrations at the point supports, the elements above the columns were made linear elastic. All material properties are given in Table 2, and mean values were employed. The tendons were given curved profiles as shown in Figure 2, and the bundles were modelled as single tendons with 2 and 3 times larger cross-sections, respectively. A post-tensioning force of 200.9 kN was applied to each tendon, and the tendons were unbonded, assuming zero friction. The post-tensioning and the self weight of the slab were applied as an initial load step, before the water pressure was applied stepwise.

The slab was meshed using quadrilateral, isoparametric curved shell elements with 8 nodes and five degrees of freedom per node; three translations and two rotations [9]. A 2x2 quadratic Gauss integration scheme was used over the area of the element, while a 7-point Simpson integration scheme was employed in the thickness direction of the slab. A relatively fine mesh of 2838 elements with approximate size 200 mm was provided to give accurate results. The tendons were inserted as embedded reinforcement bars. Element results such as stresses and strains were taken from the integration points.

3.3 Parametric study of tensile behaviour

A parametric study was performed to find an appropriate tensile stress-strain curve for implementation in the numerical analyses. The tensile curves from the sawn beams given by [10] were taken as a basis, as well as previous research such as [5]. Common for all the tensile curves from the sawn beam tests was that they displayed a distinct peak stress followed by a softening branch, before reaching a constant stress value equal to the residual tensile strength. An approximate value of $f_{ftm,res2.5} = 1$ MPa was used for the residual tensile strength in the analyses, based on the sawn beam tests, see Table 1. The tensile strengths from the bending tests ranged from approximately 3 to 5 MPa [10].

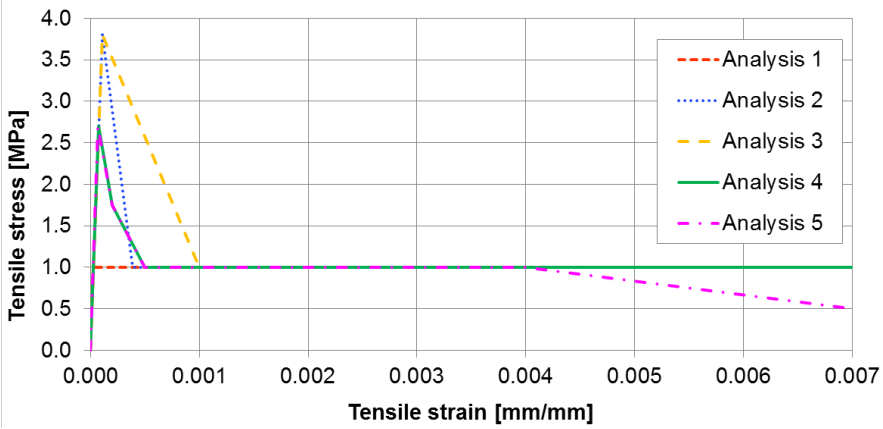

Figure 5: Tensile curves for SFRC implemented in the model

Table 3: Tensile parameters tested in the numerical study

Analysis	1	2	3	4	5
f_t (MPa)	1.0	3.8	3.8	2.7	2.7
f_2 (MPa)	1.0	1.0	1.0	1.0	1.0
ε_2 (‰)	-	0.39	1.0	0.5	0.5
f_{ult} (MPa)	-	1.0	1.0	1.0	0
ε_{ult} (‰)	-	10	10	10	10

Five different tensile curves were investigated in this study, as presented in Figure 5 and Table 3. One was a highly simplified curve with a constant curve equal to the tensile residual strength, $f_{ftm,res2.5} = 1$MPa. Two curves had a peak stress equal to the mean tensile strength, $f_{ctm} = 3.8$ MPa from [14], but different post-peak slopes, before reaching a constant residual tensile strength. The last two curves were given a characteristic tensile strength according to [14] of $f_{ctk} = 2.7$ MPa followed by a multilinear softening branch, whereas one was dragged to zero stress for the ultimate strain. The elastic modulus given in Table 2 was employed for all five alternatives.

4 COMPARISON OF EXPERIMENTAL AND NUMERICAL RESULTS

The results from the five different tensile stress-strain curves were compared to the experiment to see how the response of the model was affected. The main objective of the analyses was to capture the global response of the structure. In this section, the load-displacement curves from the various tensile models are discussed, as well as moment redistribution and axial force distribution in the slab. Finally, the failure mode of the numerical model was examined.

4.1 Load-displacement relation

The load-displacement curves from the analyses were taken from a node with the same location as LVDT 2, in the exterior span where the largest deflection occurred, see Figure 1. A comparison of all the load-displacement curves from the numerical analyses and the experimental results measured by LVDT 2 is shown in Figure 6. The analyses with the lower tensile strength of 2.7 MPa provided the best resemblance with the experimental load-deflection curve, although all models except number 3 showed relatively satisfactory results.

It is possible to optimise the tensile curves to resemble the experimental curve better, however, the aim of the study was not necessarily to find the exact load-displacement curve, but to investigate how the tensile parameters affected the response of the numerical model. In addition, it was desirable to use the results obtained from the bending tests, to find out whether they were representative for the model or not. In the following, the results from the various tensile models are shortly presented. The tensile curves are shown in Figure 5 and the respective results are presented in Figure 6.

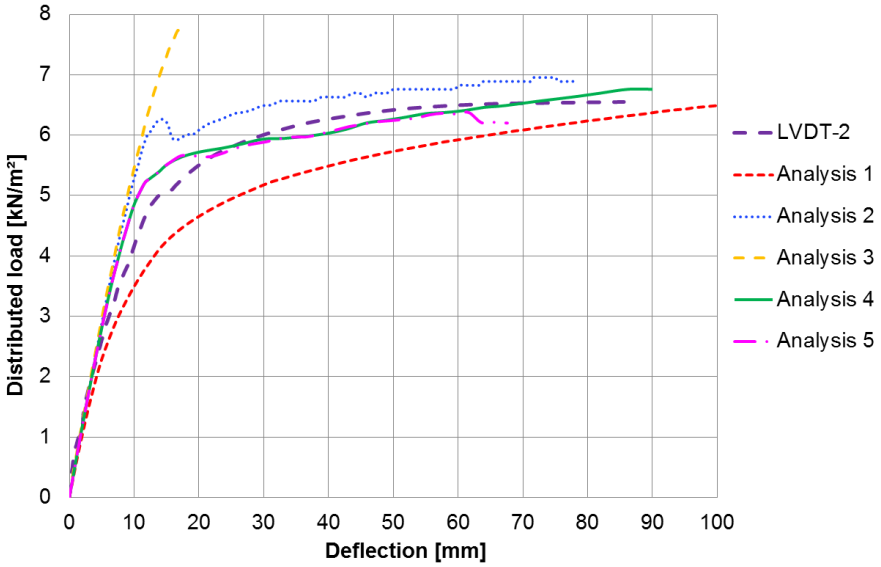

Figure 6: Load-displacement curve at midspan, all analyses

Analysis 1, using a constant tensile curve, provided relatively good results, considering the highly idealised tensile behaviour. The load-displacement curve was, as expected, too soft and without any irregularities and there was no clear sign of failure from the response curve. The shape of the load-displacement curve shows relatively good resemblance with the experimental curve, but the analysis overestimated the deflections of the slab and conservative results were obtained. For design in service limit state, this analysis could provide sufficiently accurate results, as the curve does not deviate until it enters the nonlinear area and the deviation is on the safe side.

Analysis 2 was given a tensile strength of 3.8 MPa and a negative slope of $E_{c,neg} = 10000$ MPa, a value suggested in [5]. Due to the sharp peak in this curve, obtaining convergence was problematic. The response from this analysis was too stiff, although the shape of the curve was satisfying. According to [10] the crack stress in the x-direction was reached at a load of 5.1 kN/m^2, which can be observed by a horizontal part in the experimental curve. For Analysis 2, the cracking in the span was displayed at approximately 6.2 kN/m^2, and was followed by unloading before the load increased again. The analysis was continued until it reached the same deflection as the experiment, but for the last part of the curve numerical problems occurred and this part will be disregarded in the further investigation.

Analysis 3 had a tensile curve with a tensile strength of 3.8 MPa but a more gentle post-peak slope. This implied that the strain energy of this tensile model was about twice as large as for Analysis 2, and the response curve became nearly linear. This alternative was not further investigated, but was included to show of how sensitive the model proved to be to changes in the tensile curve.

Analysis 4 was given a tensile strength of 2.7 MPa, which is lower than indicated by the bending tests, but the shape of the tensile curve resembled the bending test curves well. This analysis

showed the best correspondence with the experimental curve and it experienced less numerical problems than Analysis 2. The load-displacement curve was too stiff in the beginning, but after a displacement of 20 mm it became too soft. The load capacity of this analysis was slightly underestimated, which was expected, as the tensile strength being used was lower than the strengths taken from the bending tests. Moreover, a multilinear descending branch, as opposed to a linear, did not seem to affect the results notably.

Analysis 5 had the same tensile curve as Analysis 4, but the curve descended to zero for the ultimate strain. The response curve was similar to the curve from Analysis 4 except unloading occurred after approximately 6.4 kN/m^2, due to the added descending branch in the tensile curve. The results from Analysis 4 were not included in the further investigations.

4.2 Moment redistribution

Significant moment redistribution occurred during the experiment, most likely being one reason why the slab obtained a higher load resistance than calculated. According to [10] the most critical section was at the exterior span (see Figure 3) which was subjected to sagging moment in the x-direction. Consequently, as the capacity was reached in the span, the loads redistributed to the supports. Analyses 1, 2 and 4 were used to show the redistribution in the numerical model. In Figure 7, the distributed moments at the interior column are plotted against the water load and compared to a linear elastic analysis of the same slab model.

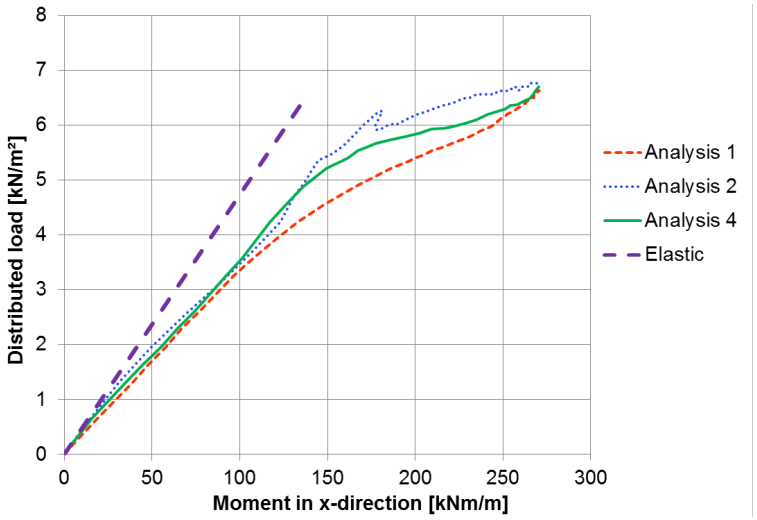

Figure 7: Moment in x-direction at interior column (support)

All the three nonlinear analyses displayed substantial moment redistribution to the supports, compared to the elastic analysis. However, the development and level of redistribution differed. Analysis 1 obtained the largest redistribution, while for Analysis 2, major redistribution occurred after cracking in the span, displayed by a dip in the curve. Analysis 4 showed something in between the other two. The values of the support moments from the analyses were unrealistically high, because the columns were modelled as point supports. For the span, the moments found from nonlinear analyses did not deviate notably from the results of the elastic analysis.

4.3 Distribution of post-tensioning forces

The distribution of axial forces from post-tensioning is of importance when designing post-tensioned flat slabs. The tendon layout used in this experiment was designed to obtain a one-way slab; it provided evenly distributed post-tensioning forces in the x-direction and concentrated forces in the y-direction.

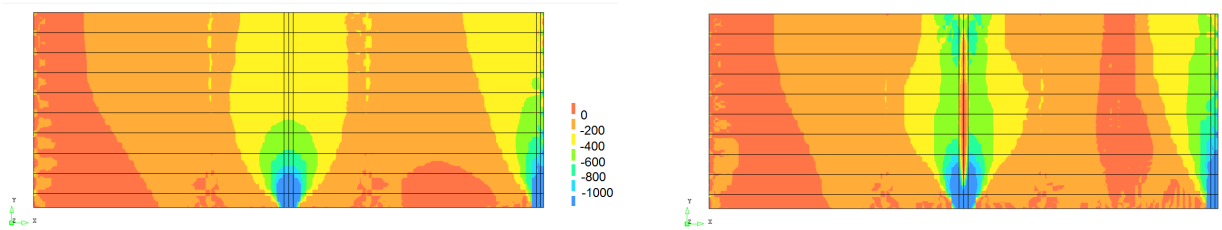

(a) $N_{yy}, q_w = 0$ *(b)* $N_{yy}, q_w = 6.1$

Figure 8: Distribution of axial forces N_{yy} in the slab [kN/m]

Figure 8 shows the distributed axial forces in the y-direction, N_{yy}, from the concentrated tendons before applying the water pressure and at failure, respectively. The results were taken from Analysis 4 and the failure load was assumed to be 6.1 kN/m^2. Figure 8(a), displaying N_{yy} due to post-tensioning only, shows that the concentrated tendons applied compression to nearly the entire slab. However, N_{yy} was highly concentrated at the anchors, where the post-tensioning was applied as an external force. During loading, N_{yy} increased above the interior column, which presumably was an effect of membrane forces in the slab caused by the water load. N_{yy} increased only in a limited area close to the tendons, as seen in Figure 8(b). The failure zones at the interior column strip and in the exterior span can also be seen in Figure 8(b), displaying zero pre-stressing in the respective zones. The axial forces in the x-direction applied by the distributed tendons, N_{xx}, were as expected nearly constant across the slab and throughout the loading scheme.

4.4 Failure mode

All the analyses were capable of displaying the failure behaviour with yield lines in the exterior span and above the interior column. Analysis 1 did not display a distinct point of failure, but for analyses 2 and 4 the failure modes were further investigated. The strains in x-direction were taken from an element with the same location as LVDT 1 (see Figure 1), at the bottom of the slab, and plotted over the load steps, see Figure 9. The results from analyses 2 and 4 show that for both models there was a clear load level at which the strains increased extensively without the load increasing, indicating that major crack propagation and eventually failure occurred. Thus the failure loads from analyses 2 and 4 were assumed to be 6.8 kN/m^2 and 6.1 kN/m^2, respectively.

The failure modes and crack patterns from analyses 2 and 4 were very similar, except for different failure loads, thus only results from Analysis 2 are included in the following. Figure 10 and 11 show the failure mode for Analysis 2, in terms of principal tensile strains and crack

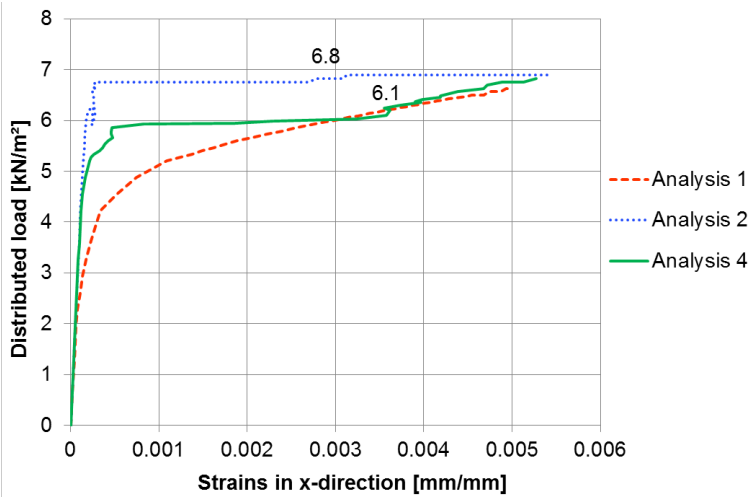

Figure 9: Strains in x-direction over the load steps, at exterior span (bottom)

patterns, respectively. From Figure 10 it can be seen that the numerical model provided the correct failure mode for the slab (see Figure 3 and 4), and by plotting the principal tensile strains, the localisation of the failure zones was clearly visualised. The plots display tensile strains larger than 0.001, which is the area in the tensile model where the fibre contribution dominates the post-cracking behaviour of SFRC and the tensile stress equals the residual tensile strength. The plots also show large strain concentrations and cracks arising around the columns, especially the interior column, but this did not initiate failure.

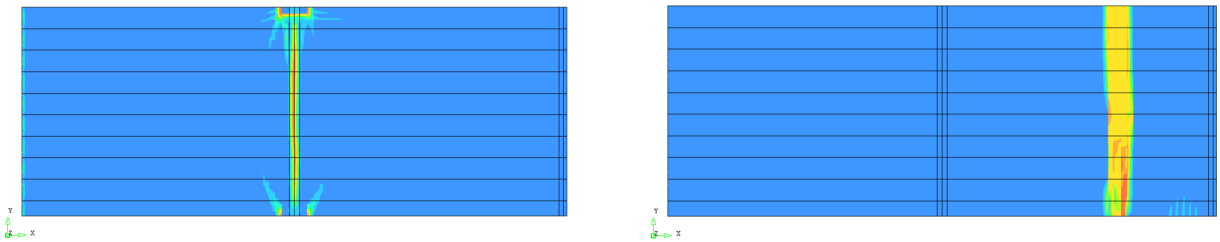

(a) Principal tensile strains at top *(b) Principal tensile strains at bottom*

Figure 10: Principal tensile strains at failure load, Analysis 2

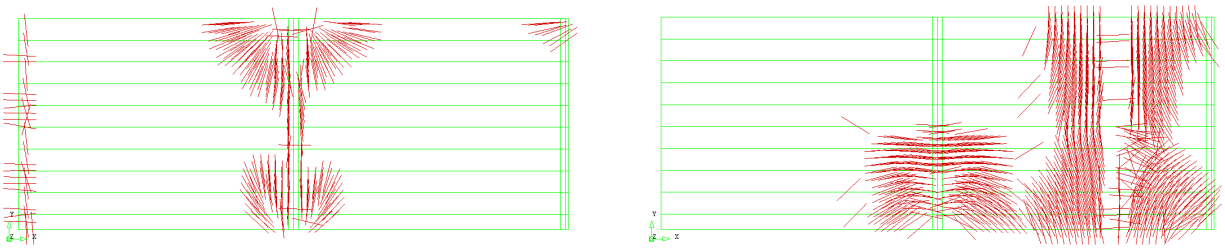

(a) Cracks at top *(b) Cracks at bottom*

Figure 11: Crack pattern at failure load, Analysis 2

When using a smeared crack model, cracks will generally be distributed over a large area, and

crack localisation may not be properly displayed if the finite elements are too large. Figure 11 shows crack patterns of the model at failure, and it is seen that the cracks are distributed over a large area and the crack patterns are not in correspondence with the plots in Figure 10. However, the crack patterns show that at failure, the large localised cracks causing the collapse of the slab had already developed (seen as areas without cracks where the yield lines were located), and crack propagation beyond these lines was present.

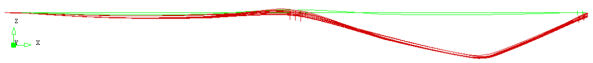

Figure 12: Deflection at failure for Analysis 2, magnified with a factor 20

The deflections from both analyses 2 and 4 were too low at failure, compared to the experiment. The experimental slab endured deflections up to 90 mm before collapsing, while the maximum deflection caused by the water load at failure was 60 mm and 43 mm for Analysis 2 and 4, respectively. When the slab in the experiment was deformed in the critical span, the water load in this area increased correspondingly, as the volume of the water increased. This effect was not included in the numerical analyses, and may be one explanation why the deflections from the analyses were too small. Also, finite element solutions tend to be too stiff, as they contain too many constraints. The deflection shape from Analyses 2 is shown in Figure 12. When comparing to the failure of the experiment, shown in Figure 4, Analysis 2 displays good resemblance and the same yield line mechanism.

5 CONCLUSIONS

The numerical model was capable of capturing the ductile bending behaviour of the slab and to display the correct failure mode, and the load-displacement curves corresponded well with the experiment. Significant moment redistribution was displayed, from the most critical section in the exterior span to the columns. Furthermore, the contribution of the steel fibre was captured by the finite element model due to the implemented tensile behaviour of the SFRC, containing the residual tensile strength. The parameter study of the tensile properties of SFRC showed that the finite element model was relatively sensitive to the tensile model, especially when the strain energy of the system was increased. However, the deviation between the response curves from the experiment and the analyses was not prominent until the nonlinear area of the load-displacement curves was entered, and for service limit state the change in tensile model had little impact. For the ultimate limit state, however, the tensile model used is of significance. The conclusions can be summarized as the following:

- The numerical model was relatively sensitive to changes made in the tensile constitutive model, especially when the strain energy was increased
- Analysis 1, having a constant tensile curve with tensile strength equal to $f_{t,res,2.5}$, provided sufficiently accurate results for service limit state and the results were on the safe side, however no distinct failure was obtained

- Except for Analysis 1, the model was too stiff and provided too low deflections at maximum load
- Significant moment redistribution was displayed by the finite element model, from the critical section in the exterior span to the interior column
- All analyses were able to capture the ductile bending behaviour of the slab and to display the correct failure mode, and the load-displacement curves corresponded well with the experiment

ACKNOWLEDGEMENT

All measurements, calculations and data from the experiment were provided by Malin Anette Hallberg and Håvard Emaus Hanssen and through their Master's thesis "Post-tensioned fibre reinforced flat slab" from June 2013 [10].

REFERENCES

[1] I. Löfgren, *Fibre-reinforced concrete for industrial construction-a fracture mechanics approach to material testing and structural analysis*. PhD thesis, Chalmers University of Technology, 2005.

[2] V. Gribniak, G. Kaklauskas, A. K. Hung Kwan, D. Bacinskas, and D. Ulbinas, "Deriving stress–strain relationships for steel fibre concrete in tension from tests of beams with ordinary reinforcement," *Engineering Structures*, vol. 42, pp. 387–395, 2012.

[3] T. Kanstad, D. A. Juvik, A. Vatnar, A. E. Mathisen, S. Sandbakk, H. Vikan, E. Nikolaisen, Å. Døssland, N. Leirud, and G. O. Overrein, "Forslag til retningslinjer for dimensjonering, utførelse og kontroll av fiberarmerte betongkonstruksjoner," in *COIN Project report no 29*, SINTEF Building and Infrastructure, COIN, 2011.

[4] T. Kanstad, M. A. Hallberg, H. E. Hanssen, and S. Trygstad, "Rik på fiber," in *Rapport - Betonginformasjonsdag 2013*, October 2013.

[5] Å. Døssland, *Fibre reinforcement in load carrying concrete structures*. PhD thesis, Norwegian University of Science and Technology, 2008.

[6] S. Sandbakk, *Fibre Reinforced Concrete: Evaluation of test methods and material development*. PhD thesis, Norwegian University of Science and Technology, 2011.

[7] A. M. Brandt, "Fibre reinforced cement-based (FRC) composites after over 40 years of development in building and civil engineering," *Composite Structures*, vol. 86, no. 1, pp. 3–9, 2008.

[8] T. Kanstad, S. Sandbakk, M. R. Geiker, and T. A. Martius-Hammer, "Flowable fibre reinforced concrete: Materials development, fibre distribution and structural properties," *Concrete Under the Northern Lights*, vol. -, pp. 60–65, 2013.

[9] TNO, *Diana User's Manual*. TNO DIANA, January 2012. Diana version 9.4.4.

[10] M. A. Hallberg and H. E. Hanssen, "Post-tensioned fibre reinforced flatslab," Master's thesis, Norwegian University of Science and Technology, 2013.

[11] KrampeHarex, "Krampeharex datasheet: Steel wire fibre with hooked ends." http://www.krampeharex.com/index.php?id=1696.

[12] J. Seehusen, "Forskalingen ga fra seg et langt, pinefullt skrik." http://www.tu.no/bygg/2013/05/27/forskalingen-ga-fra-seg-et-langt-pinefullt-skrik, May 2013.

[13] E. Thorenfeldt, S. Fjeld, *et al.*, "Stålfiberarmering i betong. Veiledning for prosjektering, utførelse og kontroll," *Høringsutkast Mai*, 2006.

[14] “Eurocode 2: Design of concrete structures: Part 1-1: General rules and rules for buildings. NS-EN 1992-1-1:2004+NA:2008,” 2008.